# Collective strong coupling with homogeneous Rabi frequencies using a 3D lumped element microwave resonator

Andreas Angerer, Thomas Astner, Daniel Wirtitsch, Hitoshi Sumiya, Shinobu Onoda, Junichi Isoya, Stefan Putz, and Johannes Majer

Citation: Appl. Phys. Lett. **109**, 033508 (2016); doi: 10.1063/1.4959095
View online: https://doi.org/10.1063/1.4959095
View Table of Contents: http://aip.scitation.org/toc/apl/109/3
Published by the American Institute of Physics

# Collective strong coupling with homogeneous Rabi frequencies using a 3D lumped element microwave resonator

Andreas Angerer,[1,a)] Thomas Astner,[1] Daniel Wirtitsch,[1] Hitoshi Sumiya,[2] Shinobu Onoda,[3] Junichi Isoya,[4] Stefan Putz,[1,5] and Johannes Majer[1,b)]
[1]*Vienna Center for Quantum Science and Technology, Atominstitut, TU Wien, Stadionallee 2, 1020 Vienna, Austria*
[2]*Sumitomo Electric Industries Ltd., Itami 664-001, Japan*
[3]*Takasaki Advanced Radiation Research Institute, National Institutes for Quantum and Radiological Science and Technology, 1233 Watanuki, Takasaki, Gunma 370-1292, Japan*
[4]*Research Centre for Knowledge Communities, University of Tsukuba, 1-2 Kasuga, Tsukuba, Ibaraki 305-8550, Japan*
[5]*Department of Physics, Princeton University, Princeton, New Jersey 08544, USA*

(Received 20 May 2016; accepted 7 July 2016; published online 21 July 2016; publisher error corrected 22 July 2016)

We design and implement 3D-lumped element microwave cavities that spatially focus magnetic fields to a small mode volume. They allow coherent and uniform coupling to electron spins hosted by nitrogen vacancy centers in diamond. We achieve large homogeneous single spin coupling rates, with an enhancement of more than one order of magnitude compared to standard 3D cavities with a fundamental resonance at 3 GHz. Finite element simulations confirm that the magnetic field distribution is homogeneous throughout the entire sample volume, with a root mean square deviation of 1.54%. With a sample containing $10^{17}$ nitrogen vacancy electron spins, we achieve a collective coupling strength of $\Omega = 12$ MHz, a cooperativity factor $C = 27$, and clearly enter the strong coupling regime. This allows to interface a macroscopic spin ensemble with microwave circuits, and the homogeneous Rabi frequency paves the way to manipulate the full ensemble population in a coherent way. 
[http://dx.doi.org/10.1063/1.4959095]

Many different approaches have been proposed for the realization of hybrid quantum systems[1–5] ranging from atoms to solid state spins coupled to microwave cavities. Most of these systems are realized by using distributed transmission-line[6] or zero-dimensional lumped element resonators (LERs),[7] which allow small confined cavity mode volumes in the microwave domain. This gives rise to strong interactions of the electric or magnetic dipole moment of a two-level system with the electromagnetic field of the cavity. In order to allow the coherent exchange of energy on the single photon level,[8–10] the coupling strength of the single-mode cavity with the two level system has to exceed all dissipation rates in the system.

The interaction strength of the cavity field with a magnetic dipole is small compared to that of an electric dipole; therefore, the interaction has to be collectively enhanced. This can be realized by an ensemble of $N$ spins in the cavity mode whose collective coupling strength is increased by a factor of[11–13] $\sqrt{N}$. Strong coupling of such large spin ensembles to one-dimensional cavities has been successfully demonstrated.[14–19] However, a big disadvantage of these cavities arises when coupling to large ensembles of emitters, because of the large magnetic field gradient of planar circuits. A macroscopic sample placed on top of such a structure is emerged in a magnetic field that changes significantly over the sample's spatial extent. This leads to a strongly inhomogeneous distribution of coupling strengths between individual spins and the cavity. The resulting inhomogeneous single spin Rabi frequencies make it impossible to manipulate and control the whole spin ensemble coherently.

A different approach is using 3D microwave cavities.[20–23] Their closed structure offers high Q values[24,25] and only negligible contributions to loss from surface two-level systems,[26] but suffer from their huge mode volume. This results in rather weak single spin coupling strengths and requires large ensemble sizes or spin systems with larger magnetic moments.[21] Some of theses issues have been addressed already and have shown promising results.[27–30]

We report the design of a 3D-lumped element microwave cavity in order to ensure large and *homogeneous* single spin Rabi frequencies. In combination with inhomogeneous broadening of the spin ensemble,[31] for which we can account for using spin-echo refocusing techniques, an inhomogeneous field distribution throughout the sample prohibits the uniform and coherent manipulation of a spin ensemble. Our design addresses this problem by making use of metallic structures to focus the AC magnetic field, such that the resulting field distribution is homogeneous throughout the mode volume while yielding large coupling rates at the same time.

In a numerical study, using COMSOL Multiphysics© RF-module, we analyze the electromagnetic field distribution inside the cavity and optimize the coupling strength for an individual spin. The cavity design is loaded with a high pressure high temperature (HPHT) diamond sample containing 40 ppm

a)Electronic mail: andreas.angerer@tuwien.ac.at
b)Electronic mail: johannes.majer@tuwien.ac.at

 

of nitrogen-vacancy (NV) spins. We reach the strong coupling limit of cavity quantum electrodynamics (QED) and open the way for new cavity QED protocols.

In cavity QED, the interaction of light and matter is enhanced by creating boundary conditions for the electromagnetic field inside a spatially confined mode volume. In the optical domain, this is usually achieved by using Fabry-Pérot-like cavities which create standing waves in free space or inside a waveguide between two mirrors. This principle can be brought to the microwave regime in different ways. The most straightforward implementation is a rectangular waveguide cavity[32] where the eigenfrequency is determined by the box dimensions with respect to the wavelength of the cavity photons. This leads to large resonators with mode volumes that are at least larger than $\lambda^3/8$ (with $\lambda$ the wavelength of the cavity photons).

Microwave electronics also uses on chip transmission line waveguides and the realization of one-dimensional microwave cavities has proven to be a powerful implementation, ranging from high efficiency single photon detection[33,34] to quantum information processing.[35,36] However, these devices and their spatial extent is always connected to the wavelength of the fundamental resonance, regardless if they are one or three-dimensional distributed.

In contrast, an electrical *LC* oscillator is created by discrete elements for capacitance $C$ and inductance $L$, for which the eigenfrequency is given by $\omega = \frac{1}{\sqrt{LC}}$. In such a lumped element resonator (LER),[7] the actual extent is not related to the wavelength of the cavity photons which allows to modify the size and shape of the cavity mode volume. This principle can also be applied to three-dimensional lumped structures.[28]

Here, we demonstrate how this can be brought one step further by using our so-called bow-tie structure within a 3D cavity. These structures not only focus on the magnetic field to a small mode volume but also make it possible to couple strongly and homogeneously to a small spin ensemble (Fig. 1(a)). The two bow-tie shaped elements are placed in a closed conducting box where the top surfaces form two large capacitors with the lid. The total capacitance of this cavity is then given by two capacitors in a series configuration reading,

$$C_{tot}^{-1} = C_1^{-1} + C_2^{-1} = 2C^{-1} = \frac{2}{\epsilon_0}\frac{d}{A}, \tag{1}$$

where $A$ is the top area of one bow-tie, while $d$ is the separation between the bow-tie and the cover lid.

The inductance $L$ is governed by the path length $l$ the current has to flow between the two capacitors in order to close the *LC* circuit (Fig. 1(b)). It can be approximated by the inductance of a flat wire conductor[37] $L_{tot} = l(\ln(l/(w+t)) + 0.5 + 0.2235((w+t)/l))$ of width $w$ as the width of the bow-tie structures and $t$ is the skin depth of the oscillating current. The resulting eigenfrequency is then given by

$$\omega_c = \frac{1}{\sqrt{L_{tot}C_{tot}}}. \tag{2}$$

We estimate the two capacitances of our system (labelled $C_1$ and $C_2$ in Figs. 1(b) and 1(c)) to have a value of 5.8 pF each. The inductances evaluate to 0.15 nH for $L_1$ and 0.8 nH for $L_2$, respectively. This yields a total capacitance of 0.95 nH and inductance of 2.9 pF with an estimated resonance frequency at 3.03 GHz.

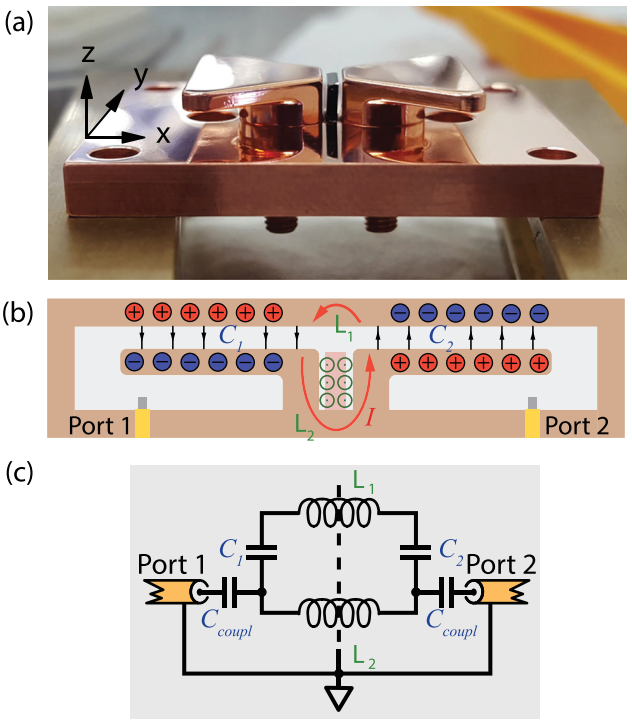


FIG. 1. (a) Manufactured cavity with mounted diamond sample. For illustrative purposes, the top lid that closes the structure and the sidewalls are not shown in this picture. (b) Schematic cross section of the cavity perpendicular to the mode direction. Capacitors and inductors are labeled as $C_1$, $C_2$, $L_1$, and $L_2$, with the electric and magnetic fields generated by the design. The current that generates the focused magnetic field is drawn as red line. The sample is drawn as shaded red rectangle. (c) Equivalent circuit for the lumped element resonator. 50 Ω terminated input and output ports are coupled via two coupling capacitors ($C_{coupl}$) to the LC circuit. Inductors and capacitors are labelled according to Fig. 1(b).

Thus, the resonance frequency of our 3D LER is only governed by the geometric values of $l$, $w$, $A$, and $d$ and not the dimensions of the enclosing box. Employing this principle, we design the cavity in a way that the distance between the bow-tie structures can be adjusted after manufacturing. With control over the inductance and capacitance, we reach a wide range of tune-ability for the resonance frequency and different sample sizes in the active region. Further, the spatial separation of electric and magnetic field makes the resonator properties insensitive to the changes of the dielectric constant in the mode volume. For a diamond placed between the two bow-tie structures, the resonance frequency and quality factor changes by less than 1%.

The electromagnetic field inside the cavity is capacitively coupled via two coaxial ports, located below the bow-tie structures. In- and out-coupling capacitances can be adjusted by changing the length of these probes, determining if the cavity is under- or over-coupled. The current is counter-propagating in the two bow-tie structures; therefore, the magnetic field between them is reinforced and focused on a relatively small mode volume. This results in an enhancement of the magnetic dipole interaction of the cavity mode with our spin system. Moreover, from numeric simulations we observe that the magnetic field is homogeneous within 1.57% in the region between the bow-tie structures when calculating the

root mean square (RMS) deviation integrated over the sample volume (see Fig. 2). The homogeneous field distribution also ensures uniform single spin coupling rates $g_0$ over the entire sample volume.

From finite element simulations, we can extract the electromagnetic field strength, energy, and distribution inside the cavity for a given input power. The resulting single spin cavity coupling rate is deduced from the total number of photons in the cavity mode, estimated by $n \approx E_{em}/\hbar\omega$. Using the magnetic field strength $\vec{B}_{rf}$ normalized by the cavity photon number $n$ as $\vec{B}^0_{rf} = \vec{B}_{rf}/\sqrt{n}$, we can infer the coupling strength of a single spin magnetic moment with the vacuum cavity mode by

$$|g_0| = \frac{\mu_B g}{2\hbar}\left|\vec{B}^{0,\perp}_{rf}\right||\vec{S}| = \sqrt{\frac{2}{3}}\frac{\mu_B g}{2\hbar}\left|\vec{B}^{0}_{rf}\right||\vec{S}|. \quad (3)$$

Here, $\vec{B}^{0,\perp}_{rf}$ stands for the perpendicular component of the vacuum magnetic field with respect to the spin principle axis, $\vec{B}^{0}_{rf}$ denotes the total vacuum magnetic field, $\mu_B$ is the Bohr magneton, $g$ is the gyromagnetic ratio, $|g_0|$ is the absolute value for the single spin coupling strength, and the factor $\sqrt{2/3}$ accounts for the angle between cavity mode vector and spin principle axis. This yields values for the single spin coupling rate of $|g_0|/2\pi \approx 70$ mHz. These coupling rates are considerably higher compared to the coupling rates of $\approx 5$ mHz achievable in a standard 3D rectangular waveguide cavity in the same frequency domain.

For our measurements, we adjust the length of the coupling ports such that the cavity is effectively under-coupled and the total quality factor $Q$ is dominated by the internal cavity photon damping rate. These cavity intrinsic losses are dominated by ohmic losses in the metallic structures, proportional to surface roughness[38] and skin-depth of the AC magnetic field. To allow external magnetic fields to Zeeman tune electron spin transitions into resonance with the cavity, we fabricate it out of oxygen free copper (99.997% purity). In order to reduce ohmic losses of the metallic structures even further, we perform a mechanical surface treatment and polish all surfaces to a roughness $<0.25\,\mu$m. This yields a quality factor of $Q = 1920$ at 1 K (see Fig. 3(a)).

Next, we load the cavity with a diamond sample containing a large ensemble of negatively charged nitrogen-vacancy

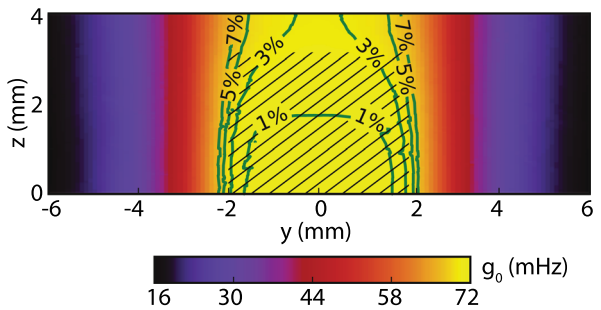


FIG. 2. Simulated magnetic field distribution. The plot shows a cross section of the mode volume parallel to the direction of the magnetic field mode (y-direction in Fig. 1(a). For the diamond sample used in this work (shown as dashed area) the deviation for the absolute value of the coupling rate is at most 7%, with a RMS deviation of 1.54%. The green contour lines divide the area in sections wherein the magnetic field strength differs by a certain percentage.

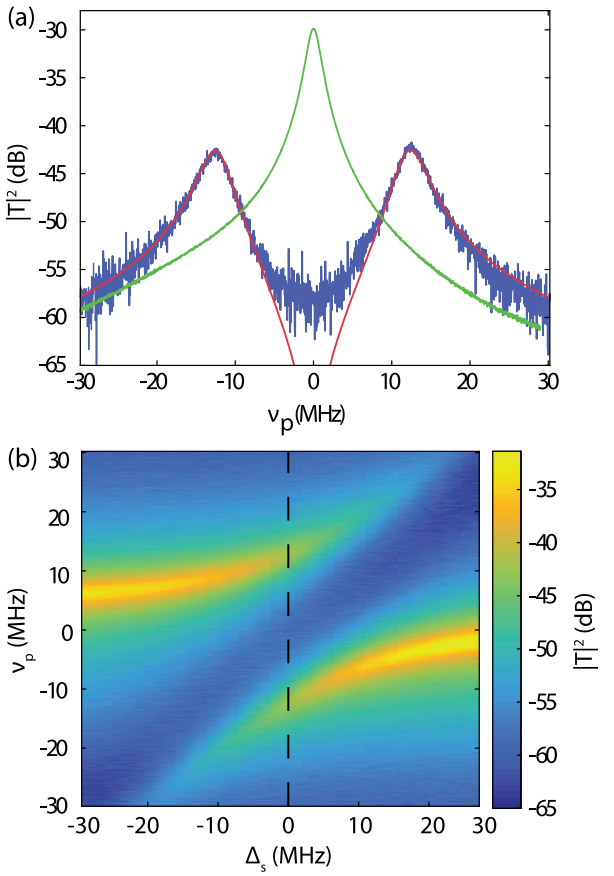


FIG. 3. (a) Transmission measurements with the spin system far detuned (*green curve*) and on resonance with an observed normal mode splitting for four NV sub-ensembles (*blue curve*). Fitting the normal mode splitting (*red curve*) with Eq. (5) yields a collective coupling strength of $\Omega/2\pi = 12.46$ MHz. (b) Cavity transmission spectroscopy as a function of $\nu_P$ versus $\Delta_s$. Here, $\nu_P$ stands for the detuning of the probe frequency relative to the spin frequency and $\Delta_s$ for the detuning of the cavity with respect to the spins. The dashed line denotes the detuning for which the normal mode splitting is measured.

(NV) defect centers. NV centers are formed by a substitutional nitrogen atom and an adjacent vacancy in the diamond lattice. Four distinct NV sub-ensembles in the diamond cell are pointing in the $\langle 1,1,1\rangle$ crystallographic direction. In the following, we use a synthetic type-Ib high pressure high temperature (HPHT) diamond with an initial concentration of 100 ppm nitrogen. The sample is irradiated with 2 MeV electrons at 800 °C and annealed at 1000 °C multiple times with a total electron dose of $1.1 \times 10^{19}\,\mathrm{cm}^{-2}$. After electron irradiation and annealing, this results in a NV concentration of approximately 40 ppm.

The electronic spin 1 ground state triplet can be described by a Hamiltonian of the following form:

$$H_{NV} = hDS_z^2 + g\mu_B\vec{B}_0 \cdot \vec{S}, \quad (4)$$

with a zero-field splitting of $D/h = 2.87$ GHz for the axial component along the NV-axes. The second term accounts for the interaction with a static external magnetic field ($\vec{B}_0$), which we use to lift the degeneracy of the $m_s = \pm 1$ manifold and tune the spin transitions into resonance with the cavity mode.

The diamond sample is glued into the cavity using vacuum grease. The (1,0,0) face is placed parallel to the direction

of the magnetic field mode ensuring the projection of the cavity mode onto the four possible NV axes to be equal. The diamond loaded cavity is mounted inside a dilution refrigerator operating at 25 mK to achieve a thermal polarization of our spin ensemble in the ground state well above 99%.

We use a vector network analyzer to probe the transmission of the coupled cavity spin system in the stationary state. The diamond loaded cavity has a fundamental resonance frequency of $\nu = 3.121\,\text{GHz}$ with a $Q$ value of 1637 and cavity linewidth of $\kappa/2\pi = 1.91\,\text{MHz}$ (half width at half maximum - HWHM). This value for the resonance frequency is in good agreement with the analytically obtained value of 3.03 GHz, with a deviation of less than 5%. With a 3D helmholtz coil configuration, we apply a homogeneous external d.c. magnetic field of approximately 12 mT on the whole ensemble in the [0,1,0] direction. This tunes all four possible NV subensembles into resonance with the cavity mode. The measured scattering amplitude $|S_{21}|^2$ is compared to an analytical expression obtained from a Jaynes-Cummings Hamiltonian reading,

$$|S_{21}|^2 = \left| \kappa \frac{(\omega - \omega_s - i\gamma^*)}{(\omega - \omega_c - i\kappa)(\omega - \omega_s - i\gamma^*) - \Omega^2} \right|^2, \qquad (5)$$

with $\gamma^*$ the inhomogeneously broadened linewidth of our spin ensemble, $\omega$ is the probe frequency, and $\omega_c$ is the cavity resonance frequency (see Fig. 3(a)). At the point where the central spin transition is in resonance with the cavity mode, we observe an avoided crossing which corresponds to a collective coupling strength of $\Omega/2\pi = 12.46\,\text{MHz}$. This is in good agreement with our simulations, assuming a homogeneous single spin coupling strength of 70 mHz and a number of spins coupling to our cavity as $\approx 10^{17}$. The number of spins can be deduced from the sample volume of 4.2 mm × 3.4 mm × 0.92 mm and an approximate NV density of 40 ppm.

The collective coupling strength is large enough to satisfy the strong coupling condition $\Omega > \kappa, \gamma^*$ with an estimated inhomogeneously broadened spin linewidth of $\gamma^*/2\pi \approx 3\,\text{MHz}$ (HWHM). It should be noted that we are neglecting effects like the cavity protection effect[39] and treat $\gamma^*$ to be a constant to the first order. This gives a cooperativity parameter of approximately $C = \Omega^2/(\kappa\gamma^*) \approx 27$.

Our results show that we are able to enter the strong coupling regime of cavity QED using our 3D lumped element cavity design. The homogeneous single spin Rabi frequency allows coherent manipulation of the whole ensemble. Spin control protocols no longer suffer from excitations diffusing out of the active region via spin-spin interaction, since all spins are emerged in a cavity mode with same field strength.

For experiments without a static external magnetic field, we carried out first measurements with superconducting cavities fabricated out of aluminum yielding quality factors up to $10^5$. They offer much higher $Q$-factors since dissipation mechanisms are only governed by AC losses in the superconducting material. As a consequence, these cavities provide higher sensitivity to emitters in the mode volume, while maintaining the advantages of large and homogeneous coupling rates.

We have presented an improved design for a 3D-lumped element resonator for cavity QED experiments. It offers high single spin coupling rates combined with a homogeneous field distribution throughout its mode volume. We fabricated the cavity out of copper, which allows Zeeman tuning the coupled spin system with an external magnetic field. These cavities already yield reasonable high $Q$-values. Even higher $Q$-values, albeit no external magnetic field tunability, are achievable when using superconducting cavities. Due to the large coupling rates of these cavities, we were able to enter the strong coupling regime of cavity QED using an ensemble of NV centers in diamond. In addition, the achieved homogeneity of the cavity field is a requirement to implement coherent spin manipulation on the whole ensemble and cavity QED protocols where this becomes important.

We thank J. Schmiedmayer, W. J. Munroe, and M. Trupke for fruitful discussions and H. Abe from the Japan Agency for Quantum and Radiological Science and Technology for assistance with electron irradiation. The experimental effort has been supported by the TOP grant of TU Wien and the Japan Society for the Promotion of Science KAKENHI (No. 26246001). A.A., T.A., and S.P. acknowledge the support by the Austrian Science Fund (FWF) in the framework of the Doctoral School "Building Solids for Function" (Project W1243). We especially thank H. Hartmann, R. Gergen, R. Flasch, A. Linzer, and W. Klikovich of the mechanical workshop of the Institute of Atomic and Subatomic Physics for technical assistance.

[1]Z.-L. Xiang, S. Ashhab, J. Q. You, and F. Nori, Rev. Mod. Phys. **85**, 623 (2013).
[2]M. Wallquist, K. Hammerer, P. Rabl, M. Lukin, and P. Zoller, Phys. Scr. **2009**, 014001.
[3]J. Verdú, H. Zoubi, C. Koller, J. Majer, H. Ritsch, and J. Schmiedmayer, Phys. Rev. Lett. **103**, 043603 (2009).
[4]A. Imamoglu, Phys. Rev. Lett. **102**, 083602 (2009).
[5]Y. Kubo, C. Grezes, A. Dewes, T. Umeda, J. Isoya, H. Sumiya, N. Morishita, H. Abe, S. Onoda, T. Ohshima, V. Jacques, A. Dréau, J.-F. Roch, I. Diniz, A. Auffeves, D. Vion, D. Esteve, and P. Bertet, Phys. Rev. Lett. **107**, 220501 (2011).
[6]M. Göppl, A. Fragner, M. Baur, R. Bianchetti, S. Filipp, J. M. Fink, P. J. Leek, G. Puebla, L. Steffen, and A. Wallraff, J. Appl. Phys. **104**, 113904 (2008).
[7]M. Hatridge, S. Shankar, M. Mirrahimi, F. Schackert, K. Geerlings, T. Brecht, K. M. Sliwa, B. Abdo, L. Frunzio, S. M. Girvin, R. J. Schoelkopf, and M. H. Devoret, Science **339**, 178 (2013).
[8]A. Wallraff, D. I. Schuster, A. Blais, L. Frunzio, R.-S. Huang, J. Majer, S. Kumar, S. M. Girvin, and R. J. Schoelkopf, Nature **431**, 162 (2004).
[9]E. Abe, H. Wu, A. Ardavan, and J. J. L. Morton, Appl. Phys. Lett. **98**, 251108 (2011).
[10]G. Boero, G. Gualco, R. Lisowski, J. Anders, D. Suter, and J. Brugger, J. Magn. Reson. **231**, 133 (2013).
[11]R. J. Thompson, G. Rempe, and H. J. Kimble, Phys. Rev. Lett. **68**, 1132 (1992).
[12]F. Brennecke, T. Donner, S. Ritter, T. Bourdel, M. Köhl, and T. Esslinger, Nature **450**, 268 (2007).
[13]Y. Colombe, T. Steinmetz, G. Dubois, F. Linke, D. Hunger, and J. Reichel, Nature **450**, 272 (2007).
[14]R. Amsüss, C. Koller, T. Nöbauer, S. Putz, S. Rotter, K. Sandner, S. Schneider, M. Schramböck, G. Steinhauser, H. Ritsch, J. Schmiedmayer, and J. Majer, Phys. Rev. Lett. **107**, 060502 (2011).
[15]Y. Kubo, F. R. Ong, P. Bertet, D. Vion, V. Jacques, D. Zheng, A. Dréau, J.-F. Roch, A. Auffeves, F. Jelezko, J. Wrachtrup, M. F. Barthe, P. Bergonzo, and D. Esteve, Phys. Rev. Lett. **105**, 140502 (2010).
[16]D. I. Schuster, A. P. Sears, E. Ginossar, L. DiCarlo, L. Frunzio, J. J. L. Morton, H. Wu, G. A. D. Briggs, B. B. Buckley, D. D. Awschalom, and R. J. Schoelkopf, Phys. Rev. Lett. **105**, 140501 (2010).
[17]C. W. Zollitsch, K. Mueller, D. P. Franke, S. T. B. Goennenwein, M. S. Brandt, R. Gross, and H. Huebl, Appl. Phys. Lett. **107**, 142105 (2015).

[18]X. Zhang, C.-L. Zou, L. Jiang, and H. X. Tang, Phys. Rev. Lett. **113**, 156401 (2014).
[19]H. Huebl, C. W. Zollitsch, J. Lotze, F. Hocke, M. Greifenstein, A. Marx, R. Gross, and S. T. B. Goennenwein, Phys. Rev. Lett. **111**, 127003 (2013).
[20]H. Paik, D. I. Schuster, L. S. Bishop, G. Kirchmair, G. Catelani, A. P. Sears, B. R. Johnson, M. J. Reagor, L. Frunzio, L. I. Glazman, S. M. Girvin, M. H. Devoret, and R. J. Schoelkopf, Phys. Rev. Lett. **107**, 240501 (2011).
[21]S. Probst, A. Tkalčec, H. Rotzinger, D. Rieger, J. M. Le Floch, M. Goryachev, M. E. Tobar, A. V. Ustinov, and P. A. Bushev, Phys. Rev. B **90**, 1 (2014).
[22]C. Axline, M. Reagor, R. W. Heeres, P. Reinhold, C. Wang, K. Shain, W. Pfaff, Y. Chu, L. Frunzio, and R. J. Schoelkopf, e-print arXiv:1604.06514 [quant-ph].
[23]Y. Reshitnyk, M. Jerger, and A. Fedorov, e-print arXiv:1603.07423 [quant-ph].
[24]H. Walther, B. T. H. Varcoe, B.-G. Englert, and T. Becker, Rep. Prog. Phys. **69**, 1325 (2006).
[25]D. L. Creedon, M. Goryachev, N. Kostylev, T. Sercombe, and M. E. Tobar, e-print arXiv:1604.04301 [physics].
[26]M. Reagor, H. Paik, G. Catelani, L. Sun, C. Axline, E. Holland, I. M. Pop, N. A. Masluk, T. Brecht, L. Frunzio, M. H. Devoret, L. Glazman, and R. J. Schoelkopf, Appl. Phys. Lett. **102**, 192604 (2013).
[27]J.-M. L. Floch, N. Delhote, M. Aubourg, V. Madrangeas, D. Cros, S. Castelletto, and M. E. Tobar, J. Appl. Phys. **119**, 153901 (2016).
[28]D. L. Creedon, J.-M. Le Floch, M. Goryachev, W. G. Farr, S. Castelletto, and M. E. Tobar, Phys. Rev. B **91**, 140408 (2015).
[29]Z. Minev, K. Serniak, I. Pop, Z. Leghtas, K. Sliwa, M. Hatridge, L. Frunzio, R. Schoelkopf, and M. Devoret, Phys. Rev. Appl. **5**, 044021 (2016).
[30]M. Goryachev, W. G. Farr, D. L. Creedon, Y. Fan, M. Kostylev, and M. E. Tobar, Phys. Rev. Appl. **2**, 054002 (2014).
[31]D. O. Krimer, S. Putz, J. Majer, and S. Rotter, Phys. Rev. A **90**, 043852 (2014).
[32]M. D. Pozar, *Microwave Engineering*, 4th ed. (John Wiley & Sons, 2011), p. 720.
[33]A. E. Lita, A. J. Miller, and S. W. Nam, Opt. Express **16**, 3032 (2008).
[34]Y. Kubo, I. Diniz, C. Grezes, T. Umeda, J. Isoya, H. Sumiya, T. Yamamoto, H. Abe, S. Onoda, T. Ohshima, V. Jacques, A. Dréau, J.-F. Roch, A. Auffeves, D. Vion, D. Esteve, and P. Bertet, Phys. Rev. B **86**, 064514 (2012).
[35]B. R. Johnson, M. D. Reed, A. A. Houck, D. I. Schuster, L. S. Bishop, E. Ginossar, J. M. Gambetta, L. DiCarlo, L. Frunzio, S. M. Girvin, and R. J. Schoelkopf, Nat. Phys. **6**, 663 (2010).
[36]R. Barends, J. Kelly, A. Megrant, A. Veitia, D. Sank, E. Jeffrey, T. C. White, J. Mutus, A. G. Fowler, B. Campbell, Y. Chen, Z. Chen, B. Chiaro, A. Dunsworth, C. Neill, P. O'Malley, P. Roushan, A. Vainsencher, J. Wenner, A. N. Korotkov, A. N. Cleland, and J. M. Martinis, Nature **508**, 500 (2014).
[37]B. C. Wadell, *Transmission Line Design Handbook* (Artech House, 1991).
[38]L. Proekt and A. C. Cangellaris, in *Proceedings of the 53rd Electronic Components and Technology Conference* (2003) pp. 1004–1010.
[39]S. Putz, D. O. Krimer, R. Amsüss, A. Valookaran, T. Nöbauer, J. Schmiedmayer, S. Rotter, and J. Majer, Nat. Phys. **10**, 720 (2014).